GESS

GLOBAL.EARTHQUAKE.SATELLITE.SYSTEM

A 20-YEAR PLAN TO ENABLE EARTHQUAKE PREDICTION

MARCH 2003

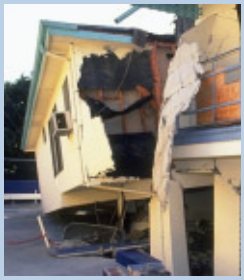

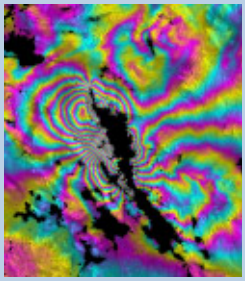

Geosynchronous Architecture

CHAPTER FOUR

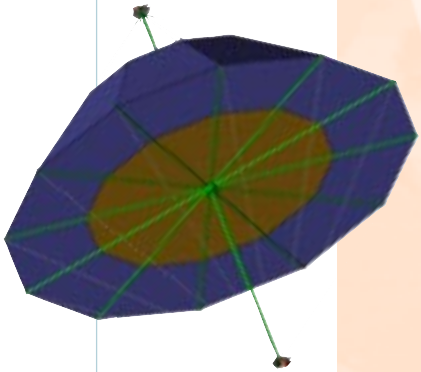

The most ambitious concept of the GESS study entails the operation of a geosynchronous SAR constellation. While the deployment of such a constellation would be a massive undertaking and require that major technological challenges be overcome, a constellation of high-altitude SAR satellites would offer advantages over lower-altitude sensors in the contexts of system operational flexibility and instantaneous accessibility of target areas on the ground (Figure 4.1). A system with such capabilities might be considered as a mission for the next decade.

Geosynchronous orbits are unique because their orbital periods are equal to one Earth day. A geostationary orbit is a special kind of geosynchronous orbit in which the orbital inclination is zero; viewed from the rotating Earth, a satellite in a geostationary orbit appears to remain fixed in the same position in the sky at all times. This property makes geostationary orbits ideal for such applications as communications and meteorology, but it in fact makes them unusable for SAR missions. This is because the principle of aperture synthesis — the very principle for which SAR is named — requires relative motion between the sensor and the scene under observation. When such motion exists, as it does for an inclined geosynchronous orbit, however, fine resolution can be obtained even from very great distances. Although a geosynchronous satellite follows an elliptical trajectory as dictated by Kepler's laws of motion, due to the relative motion of the Earth and the satellite, the nadir point traces out a "figure-8" pattern on the ground once per day (see Figure 4.2). Since radar instruments can also acquire images both during the day and at night, and unaffected by cloud cover, a high-altitude SAR constellation may be well suited to the task of 24-hour global hazard monitoring. Most of the Earth's surface could be kept in view nearly continuously by a constellation of geosynchronous satellites.

System Parameters

A geosynchronous SAR at an altitude of about 35,800 km would be more than an order of magnitude farther from the Earth than any SAR mission to date. While this high-altitude vantage point would allow a geosynchronous SAR to view a large ground area, it would also require a large physical antenna and a great deal of transmitted power. The antenna size requirements are driven by the need to resolve the range-Doppler ambiguities that are inherent in a pulsed radar system; the power requirements are driven by signal-to-noise ratio (SNR) considerations.

We envision a system with a 30-m-diameter L-band aperture antenna that transmits 60 kW of peak power over relatively long 1-ms pulses. The boresight of this antenna would be kept pointed in the nadir direction and the beam steered electronically to look either left or right. Any part of the sensor footprint could be illuminated with no more than ±8° of electronic steering — from this altitude, the limb of the Earth is only 9° from nadir. Data could therefore be acquired for areas between 1000 and 6500 km ground range from nadir on either side of the platform ground track, corresponding to ground-incidence angles of 10.6–66.4°. The antenna could also be steered to areas with ground squint angles up to ±60° on either side of the ground track with less than ±8° of electronic steering in the azimuth direction.

With such a wide swath, some of the system parameters would have to change a great deal between the near range and the far range. The bandwidth of the system might vary between 80 MHz at the steepest incidence angles to 10 MHz further out. A split-spectrum approach might be employed as in the LEO+ case in order to characterize the effects of the ionosphere. The signal polarization might also change over the sensor footprint. We envision that the spacecraft would be yaw steered to keep the antenna in a nominal HH polarization state for broadside acquisition geometries, implying that the polarization state would be mixed in squinted geometries.

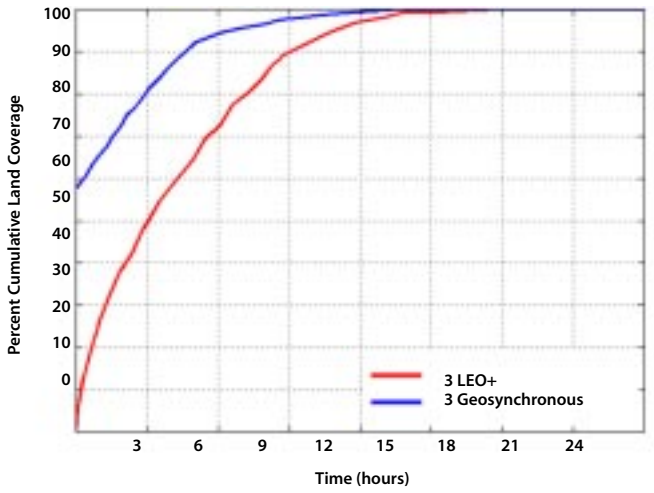

Figure 4.1
Cumulative land coverage from both LEO+ and GEO constellations of three satellites. The GEO constellation achieves over 90% land coverage in approximately half the time of the LEO+ constellation.

Figure 4.2
Trace of a geosynchronous satellite at a 60° orbit inclination (shown as figure-8). Instantaneous field of view for a 5500-km SAR swath is also shown.

Other system parameters would change over the platform orbit as the velocity of the platform relative to an observer on the Earth varies. For an orbital inclination of 60°, the relative velocity of the satellite would vary by a factor of two between about 1500 m/s when the satellite is at high latitudes and 3000 m/s when it is over the equator. The pulse repetition frequency (PRF) of the system would therefore vary between about 125 Hz and 250 Hz. Relevant system parameters are summarized in Table 4.1. Note that these relative velocities and PRFs are significantly lower than those of LEO systems.

Orbit, Coverage, Constellation

Although a geosynchronous SAR would have a very large footprint, its "figure-8" ground track would always remain in a fixed set of longitudes. A single geosynchronous sensor would consequently be unable to provide global coverage on its own. While the longitude-locked behavior of a geosynchronous SAR might prove advantageous if the mission objective were to provide coverage only of the Western hemisphere, the aim of this study has been the development of system whose scope is global. Consequently, we concentrate here on the use of multiple geosynchronous sensors.

One architecture would be a constellation of ten satellites divided into five groups of two (Figure 4.3). The two satellites in each group would follow the same ground track and would be phased 180° apart, resulting in an interferometric repeat time of 12 hours. In

Table 4.1
Geosynchronous parameters.

ORBIT	
Altitude	35788 km
Inclination	60°
Interferometric Repeat Period	1 day
VISIBLE SWATH	
Look Angle	± 1.6–8.0°
Ground Incidence Angle	±10.6–66.4°
Ground Range From Nadir	±1000–6500 km
Slant Range	35892–39224 km
Ground Squint Angle	±60°
Footprint Area	79,000,000 km^2
Subswath Width	400 km nominal
INSTRUMENT	
Antenna Diameter	30 m
Electronic Steering	±8° in azimuth and elevation
Wavelength	24 cm (L-band)
Polarization	varies with squint angle
Peak Transmit Power	60 kW
Pulse Duration	1 ms
Bandwidth	10–80 MHz
Pulse Repetition Frequency	125–250 Hz
PERFORMANCE	
Ground Range Resolution	20 m nominal
Stripmap Azimuth Resolution	varies over orbit (2–20 m nominal)
Nominal SNR	10 dB
Nominal Range Ambiguity Level	–30 dB
Nominal Azimuth Ambiguity Level	–20 dB

our initial analyses, we assume that the five groups would be equally spaced in longitude, though in an optimized constellation design, the groups might be unevenly spaced for better performance over high-priority areas. Each satellite would be in a nearly circular geosynchronous orbit with a 60° inclination.

At any given time, this ten-satellite constellation would have about 80% or more of the Earth's surface in view. Approximately 20% of the surface would be in view of one or more satellites continuously, and approximately 80% of the surface would be in view nearly continuously (about 90% of the time). Gaps in coverage would be less than one hour for about 70% of the surface to less than five hours for 100% of the surface. The areas associated with longest gaps in coverage would be located mainly near the poles and at certain longitudes near the equator. For a great majority of the Earth, a 20-m resolution image could be acquired on average within 10 minutes of an emergency event.

The 3-D displacement accuracy of the system would be excellent (Figure 4.4). Because the antenna beam could be squinted both forward and backward via electronic steering, data could be acquired from a great diversity of viewing angles. Moreover, because a target area could be viewed for long periods of time, a great deal of data could be acquired of this area, albeit at the expense of acquiring data of other areas. Typically, hundreds of images of a target area could be acquired during each interferometric repeat cycle. These data could be combined in a least-squares estimation procedure in order to reduce noise induced by

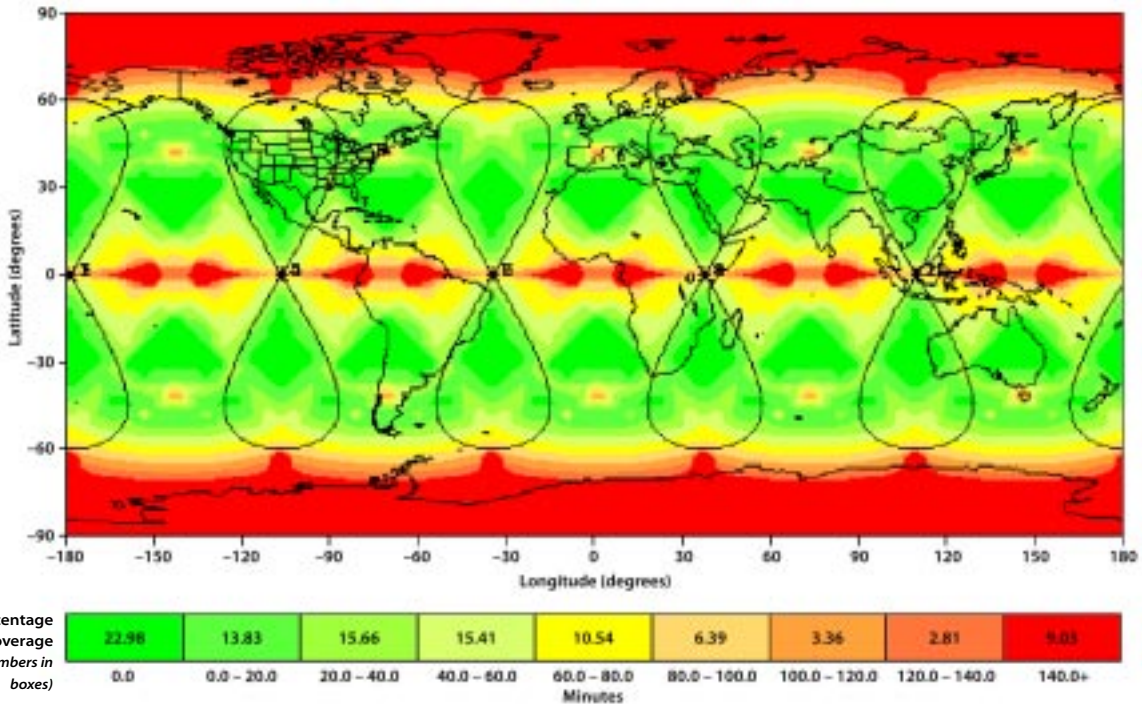

Figure 4.3
The maximum revisit time for a constellation of ten GEO satellites, five ground tracks, 12-hour phasing, at an inclination of 60°.

temporal decorrelation and tropospheric and ionospheric effects. We expect that 3-D displacement accuracies of a few millimeters could be achieved in 24–36 hours.

Instrument Modes

Most of the time, full-resolution capability would not be required. Rather, the instrument might instead be operated in various interferometric ScanSAR modes that could yield data over swaths thousands of kilometers wide (each subswath would be up to 400 km wide). Because the antenna beam would be electronically steered exclusively, data could even be acquired from nonadjacent subswaths-perhaps on opposite sides of the ground track-or from beams squinted both forward and backward. The large antenna footprint would make ScanSAR ground patches hundreds of kilometers wide in the along-track dimension. Moreover, with ScanSAR bursts up to several minutes long, the instrument operation could easily be timed well enough for repeat-pass ScanSAR interferometry. Alternately, the instrument could operate in a standard stripmap mode, or the antenna beam could be steered to dwell on particular areas of interest in a spotlight mode so that large amounts of high-resolution data from various viewing angles could be collected over key seismogenic areas. Between these different modes, the instrument would allow great flexibility in operation.

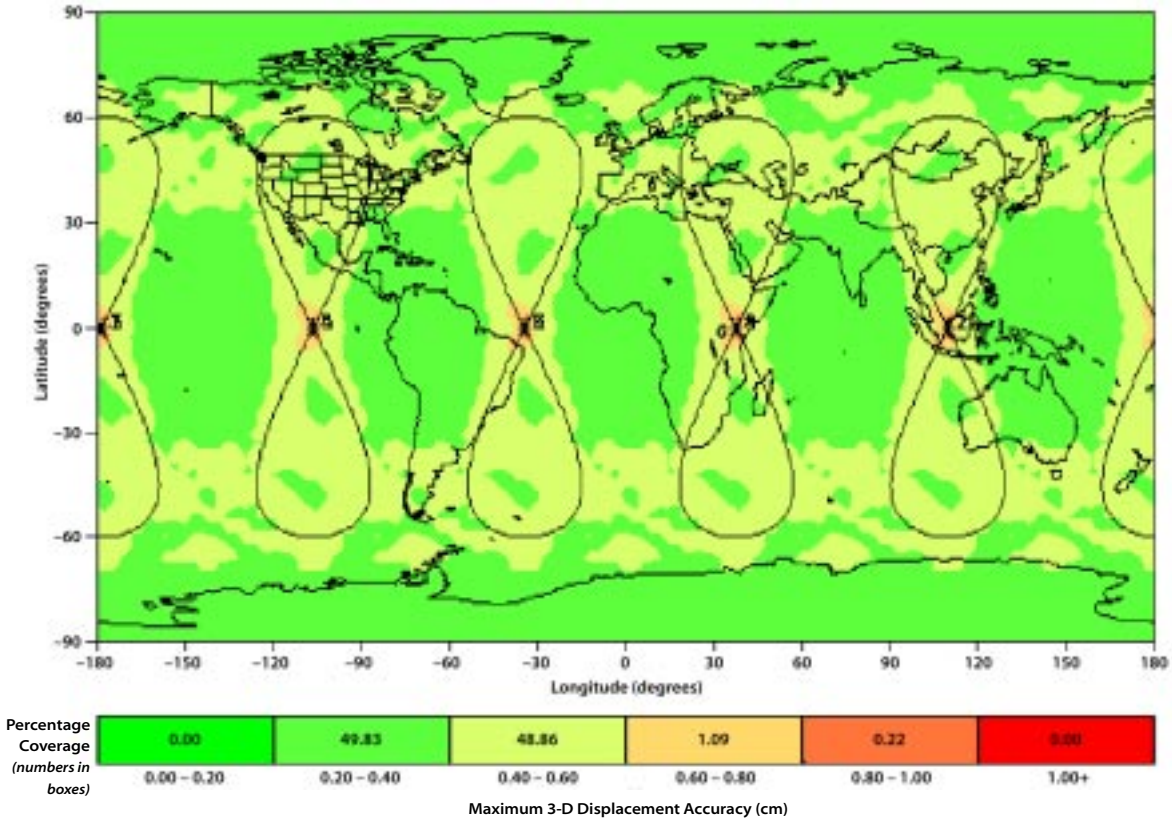

Figure 4.4
Worst-case component of the 3-D vector displacement accuracy for a constellation of ten geosynchronous SAR satellites. The units are relative to the single-image line-of-sight displacement accuracy. For each satellite pass, an image is assumed to have been acquired of the visible ground points every 30° in ground-point azimuth.

The system might have numerous modes that are tailored to different situations and changing priorities. A typical operational plan might involve the daily or twice-daily creation of multiple maps of certain high-priority seismogenic areas (as described in the LEO+ scenario) as well as low-resolution global maps every few days, or high-resolution global maps every few weeks. The operational plan could also be modified as needed in response to global hazard events and current conditions.

Performance

Because the curvature of the relative platform motion changes a great deal over the orbit, the stripmap-mode azimuth resolution depends on the satellite latitude and location of the target in the sensor footprint. When the instrument is looking towards the outside of each loop in the figure-8 pattern, the stripmap-mode azimuth resolution can be as coarse as 20 m, yet it can be finer than 2 m when the instrument is looking towards the inside. That is, in some cases, the orbit curvature would effectively cause the antenna beam to dwell on a particular ground area in a manner similar to that of a spotlight-mode SAR acquisition, even when the antenna beam is kept pointing toward broadside. Azimuth resolutions of around 2 m or better might also be obtained anywhere in the swath or along the orbit when the instrument is operating explicitly in spotlight mode.

The processing involved for attaining 2-m resolution would not be trivial, however. The required synthetic aperture length for such a resolution would be more than 200 km, over which the curvature of the platform motion would change significantly. In fact, a different azimuth-compression reference function would be required for each along-track sample position. Moreover, the slant-range depth of focus might be even smaller than the nominal slant-range resolution of around 10–20 m if 2-m resolution is desired. Another difficulty of high-resolution processing would be posed by the variability of the ground scene and of the atmosphere over the time required by the satellite to traverse the long synthetic aperture distances; up to 25 min may be required in some situations. In practice, 2-m resolution may be very difficult to achieve, though 5–10-m azimuth resolutions should be readily attainable. Note that while fine spatial resolution is not always required for geophysical applications, high-resolution data can be averaged spatially in order to mitigate the effects of temporal decorrelation in interferometric data.

Indeed, as in the LEO+ case, we expect that the interferometric displacement accuracy will be limited more by temporal decorrelation as well as by tropospheric or ionospheric effects than by the instrument performance. Given the large amount of data that a geosynchronous system can acquire of a targeted area over a short period of time, though, it is not unreasonable to expect that with sufficient averaging, the displacement accuracy can be reduced to the level of a few millimeters for specific target sites. Over larger areas, we expect that subcentimeter displacement accuracies would be typical.

The instrument would also allow for excellent 3-D displacement accuracy over much of the Earth since most points on the ground could be imaged from diverse sets of

viewing angles. This diversity of viewing angles comes from the both the lateral curvature of the ground track as well as the variation in ground squint angles that are possible through electronic beam steering from high altitudes.

Data Rates and Volume

Although the footprint of a geosynchronous SAR's accessible area would be much larger than that of a sensor in a lower orbit, the instantaneous data rates of the two would be comparable (on the order of 100–200 Mbs). This is because neither sensor would be able to acquire full-resolution data over its entire footprint simultaneously; data would need to be collected over smaller subswaths. While the subswaths of a geosynchronous SAR would be considerably wider than those of a LEO SAR, the Earth-relative velocity is slower. Despite comparable data rates, because the geosynchronous sensor is almost always in sight of land, even when the sensor itself is over water, the instrument could acquire data nearly continuously. The total data volume could therefore be on the order of 1–2 TB per satellite per day, or around 5–10 PB per satellite over the satellite's relatively long 15-year life. These values would increase by a factor of two or four if multiple radar polarizations were used.

Such data rates and volumes would require specialized downlink and data-handling facilities. Since geosynchronous satellites would be in view continuously from low-latitude ground stations for long periods of time, however, one or two dedicated ground stations could be used to downlink the data from each satellite or each pair of satellites in the same ground track. Furthermore, with appropriate intersatellite communication, one or two ground stations might be able to handle all of the data from an entire constellation.

Geosynchronous SAR Payload Description

The geosynchronous SAR instrument is dominated by the very large deployable antenna. Because of the large antenna area, our mission concept integrates the SAR antenna with the spacecraft structure and subsystems as illustrated in Figure 4.5. The 30-m-diameter antenna aperture is deployed with horizontal booms and then tensioned to maintain flatness with two asymmetric axially deployed masts and tensioning cables. The antenna aperture is constructed from flexible membrane material that is integrated with the active electronics for proper beam formation and transmit/receive signal amplification. The antenna flatness must be maintained to within 1/20 of a wavelength, or roughly 1 cm across the entire aperture. This type of flatness requirement can be achieved using the axial booms and membrane tensioning cables.

Due to the challenge of such a flatness requirement, the proper calibration of the full array is essential for successful beamforming. The principal array error sources include feed errors caused by variations in electronic components, and element displacement caused by mechanical deformation of the array surface. The removal of displacement errors is somewhat problematic. Only an external calibration system can address the problem of element displacement. There is a trade-off between mechanical rigidity (and thus, surface accuracy) and mass. In order to minimize the launch mass, it is desirable to tolerate greater

surface errors. The added complexity of an external calibration system must be weighed against the benefit of lighter structural elements. There are several approaches to external calibration. An onboard metrology system (either optical or RF) can be used. Feed errors include all (manufacturing, thermal or aging related) amplitude and phase errors in feed networks, interconnects and T/R modules. There are several proven approaches to compensating for feed errors using loop-back calibration loops. If the feedback paths are properly designed to eliminate leakage from adjacent elements, this calibration can be performed continuously during normal radar operation.

Thin-film solar arrays provide power to the antenna and spacecraft. These arrays are an integral part of the system configuration and share the same structural elements. One solar array is an annular ring formed around the perimeter of the radar antenna aperture. Solar arrays also partially cover the rear or zenith-pointed side of the spacecraft, stretching up the tensioning cables as shown in Figure 4.5. The solar array "tent configuration" provides a large surface area for solar power collection from any sun orientation but will also result in high solar pressure on the solar arrays making station keeping more challenging and costly. To minimize the effect, we have lengthened the axial boom for steeper angles of the rear-facing solar array. We have also reduced the size of the solar arrays as much as possible. The top of the solar array "tent" is open because the thermal subsystem requires a window to space for radiating excess thermal energy. The power system also includes sufficient batteries to operate for short periods in eclipse. On the tips of each mast are propulsion modules for orbit maintenance. The antenna is mounted

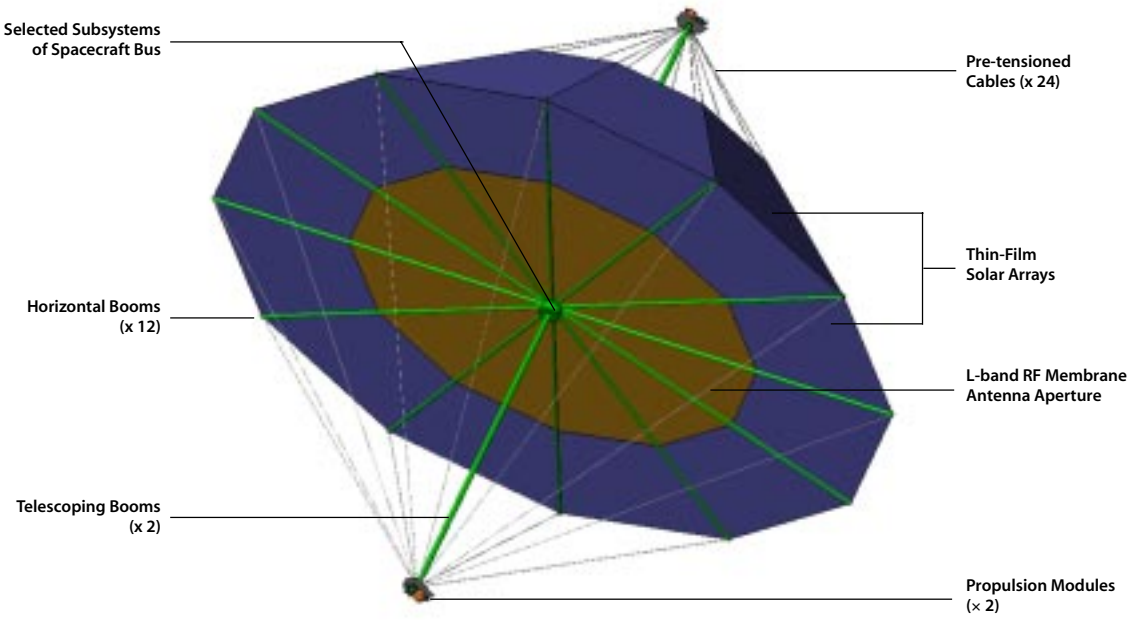

Figure 4.5
Geosynchronous SAR large deployable antenna concept.

to a centralized spacecraft bus that also houses the radar central processor/controller.

The high-radiation environment of the geosynchronous orbit poses a substantial risk to the SAR electronics, and degrades the performance and reliability of the solar arrays. Long-term exposure can cause device threshold shifts, increased power consumption, and device damage. Radiation-hardened devices and shielding can mitigate total dose effects. The expected total dose for a 15-year mission behind 30 mils of aluminum is 15 Mrad for a geosynchronous orbit inclined to 60°. Clearly, this presents a major technical challenge. The total dose decreases exponentially with shielding, and therefore the expected total dose behind 100 mils of aluminum is reduced to 600 krad. This becomes a more manageable problem. However, only limited shielding can be employed for the electronics on the antenna. Greater levels of shielding will be very massive and bulky, and perhaps not compatible with membrane antenna technology. Therefore, we consider the radiation environment to be one of the biggest challenges to realizing this system.

A more detailed description of the radar system architecture and antenna design will be presented in Chapter 6. The spacecraft bus contains the subsystems required to perform all spacecraft housekeeping functions and radar control and data handling functions. The bus also supports the deployable booms, masts, antenna aperture, and solar arrays. Twelve horizontal booms deploy, support, and tension the antenna aperture and solar array. These booms each have a fully deployed length of 19 m and are supported by, as well as stowed for launch in, the spacecraft bus. Self-rigidizable spring-tape-reinforced (STR) inflatable booms of 10 inches (0.25 m) in diameter were selected as the baseline booms. Two high-stiffness, telescoping Able Deployable Articulated Masts (ADAM) developed by AEC-Able provide axial support for the large antenna and solar arrays. The masts will be deployed axially from the top and the bottom of the spacecraft bus. The masts are asymmetric; the nadir-pointing mast has a fully deployed length of 19 m and the upper mast used to support the solar arrays has a length of 38 m. This configuration was chosen to maximize solar array efficiency and to reduce mass and solar pressure effects. Each ADAM mast has a linear mass density of 1.3 kg/m and is stowed in a dedicated canister for launch. The canister for stowing the upper ADAM mast also acts as the central mandrel for packing the antenna aperture. This means that the membrane aperture will be wrapped around the upper canister for launch. The antenna aperture is formed by three layers of thin-film membranes. The 30-m-diameter membrane antenna aperture is integrated with all of the distributed transmit, receive, and control electronics including T/R modules, true-time-delay (TTD) digital transceivers, power converters, and signal-distribution and interconnect technologies. Twenty-four pre-tensioned cables are used to stiffen the horizontal booms. The upper ADAM mast supports 12 of these cables, and the lower ADAM mast supports the other 12 cables. The solar arrays that provide all power for the instrument and spacecraft housekeeping functions are made with flexible, amorphous thin-film technology that is 13% efficient. The areal mass density of these solar arrays

is assumed to be about 0.63 kg/m^2. The front annular-ring-shaped solar array will be packaged for launch and deployed in space together with the membrane antenna aperture. The rear arrays will be deployed and supported by the 12 upper cables. Two propulsion modules are located at the tips of the ADAM masts. Each propulsion platform consists of hydrazine thrusters, solar-electric ion propulsion engines, and supporting elements of the propulsion subsystem.

The total dry mass of the integrated geosynchronous SAR flight system is roughly 4500 kg (with contingency). A breakdown of mass and power is provided in Table 4.2.

The geosynchronous SAR integrated flight system will be packaged for launch as shown in Figure 4.6. The total launch stack height is 8 m, which will fit in a Delta IV fairing. The large antenna must be stowable with high packaging-efficiency in order to physically fit into the spacecraft launch vehicle. Since low mass and low stow-volume are driving requirements, a flexible membrane antenna architecture was selected. Rigid honeycomb panels, such as that used for SIR-C and SRTM antennas, were not considered due to their larger mass and stowage volume.

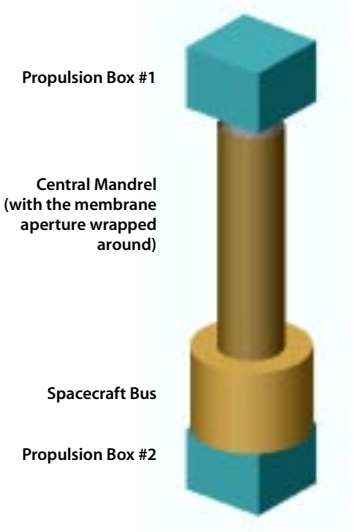

Figure 4.6
Major components of a GEO SAR flight system.

Mission Design

Because of the large area of the antenna, our concept of the mission involves the integration of the antenna and the spacecraft structure as just described, with rigidizable booms, deployed radially as illustrated in Figure 4.7. An alternative, more-traditional design involving a separate articulated solar array was examined but not selected because of the mechanical problems involved. The solar arrays of the current working design are sized such that sufficient power would be available regardless of the satellite orientation with respect to the Sun. The spacecraft would also carry enough battery capacity for three minutes of instrument operation during eclipse. This would allow images with azimuth resolutions of 10 m or better to be obtained in emergency situations if necessary. Eclipses would occur once per day during each of two month-long seasons per year, with eclipses of up to 70 minutes duration. The large central opening in the solar arrays over the back of the radar antenna aperture is required for the radiators that would provide thermal control.

Gimbaled propulsion units with both chemical and ion thrusters as well as their propellant tanks would be located on azimuthally rotating platforms at the ends of the main masts. These thrusters would be used for orbit maintenance and for dumping the built-up momentum of the reaction wheels used to provide attitude control and yaw steering. The reaction wheels themselves

Table 4.2
Geosynchronous SAR mass and power estimate.

SYSTEM/SUBSYSTEM	NO. OF UNITS	UNIT POWER (W)	TOTAL POWER (W)	UNIT MASS (kg)	TOTAL MASS (kg)
Spacecraft			**8226**		**2810**
Spacecraft Bus	1	1091	1091	1166	1166
Flex Solar Array	12	158	1894	76	909
Batteries	2	0	0	214	428
Propulsion Modules	2	2621	5241	154	307
Radar Antenna Structure			**0**		**387**
Antenna Membrane Aperture	36	0	0	4.242	152.7
ADAM Mast (nadir)	1	0	0	24.7	24.7
ADAM Mast (zenith)	1	0	0	49.4	49.4
Able Mast Canisters	2	0	0	20	40
Horizontal Boom	12	0	0	9.5	114
End Cap	24	0	0	0.25	6
Radar Electronics			**28050**		**286**
Central Processor (CPU)	1	1000	1000	25	25
Digital Receivers	61	50	3050	0.1	6
T/R Modules	15616	2	24000	0.006	94
Feed Probes/Interconnects	15616		0	0.001	16
Optical Fiber Distribution	1		0	30	30
Power Distribution Cabling	1		0	90	90
Power Converters	244		0	0.1	25
Spacecraft Total (Dry)			36276		3482
Contingency (30%)			10883		1045
Spacecraft Total (Dry) with Contingency			**47159**		**4527**
Propellant					752
Star 48 V engine for orbit circularization					2455
Launch Mass					**7734**
Launch Vehicle Capability (Delta IV 4050 Heavy) to GTO					**11000**
Launch Mass Margin (30%)					**3266**

Figure 4.7
The geosynchronous SAR flight system will undergo a four-step deployment sequence:

1. The system is separated from the fairing of the launch vehicle. See Figure 4.7(a) and (b).

2. The 12 horizontal booms and the two ADAM masts deploy. See Figure 4.7(c). The 24 tensioning cables also deploy simultaneously with the ADAM masts. These cables will be tensioned to a pre-determined level when the masts are fully extended.

3. The membrane antenna aperture, together with the annular front solar array, start to deploy by the actuation of a set of wire and pulley mechanisms. The various stages of this deployment process are illustrated in Figure 4.7(d) and (e). The fully deployed membrane aperture and ring-shape solar array can be seen in Figure 4.7(f).

4. The rear solar arrays are deployed by a second set of wire-and-pulley mechanisms. Figure 4.7(g) shows the half-deployed cone-shaped solar array and Figure 4.7(h) shows the fully deployed array. It should be noted that in these two figures a full cone is shown for this array; however, the current baseline design uses only a partially filled configuration.

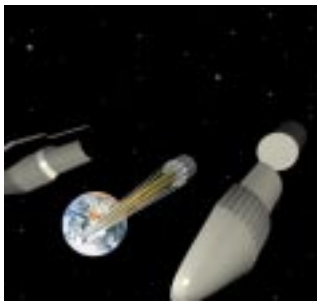
(a) Ejection from the fairing.

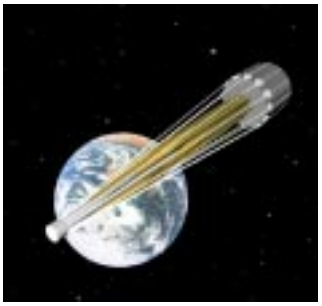
(b) Ready to deploy.

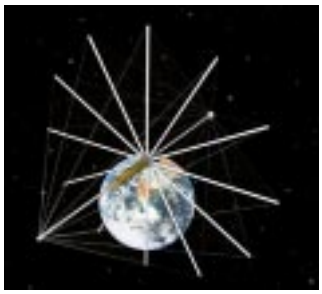
(c) Booms and masts deploy.

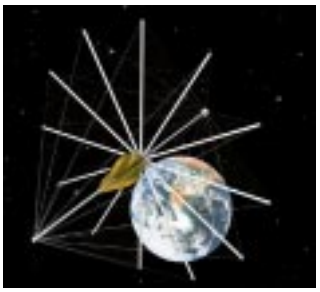
(d) Unrolling of membrane aperture.

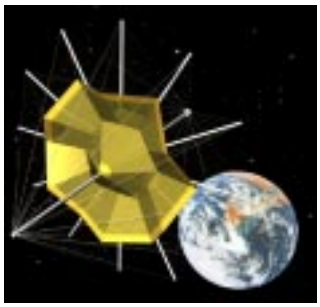
(e) Deploying membrane aperture.

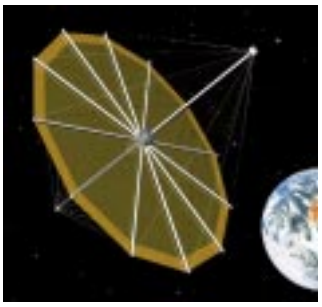
(f) Fully deployed aperture.

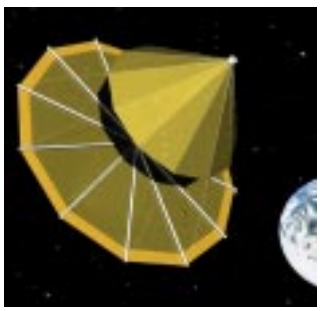
(g) Deploying cone-shaped solar array.

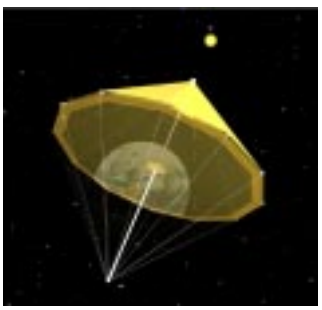
(h) Deployed GESS system.

would be located near the spacecraft center of mass. Also located at the end of the nadir mast would be a telecommunications package, including a high-gain antenna, and an Earth sensor for attitude control. The packages located here would be relatively small compared to the size of the radar antenna, so they would not interfere with the operation of the instrument. Precise knowledge of the platform position and attitude would be obtained from the Earth sensor, Sun sensors, star trackers, and a reverse GPS system.

Aside from the technological difficulties posed by the instrument, several key issues need to be addressed in the overall mission design. Because of the great distance of the radar from the Earth and the consequent need for large amounts of power (up to 37 kW DC total for the spacecraft, including 28 kW for the instrument, in addition to power for telecom, solar-electric ion propulsion, but not including contingency), a large area would be required for the solar arrays. Not only would the solar arrays constitute a large fraction of the total spacecraft mass, they would present a large surface area over which solar pressure would exert forces that perturb the spacecraft trajectory and attitude. Several thruster fires per day would be needed to maintain orbit control tightly enough for high-precision repeat-pass interferometry. It is not clear how thruster firings, whether chemical or electric, would affect the flatness of the radar antenna and the subsequent system performance.

The spacecraft mass, including contingency, would be around 4500 kg. In order to maintain an adequate launch vehicle margin of 30%, we require a launch vehicle such as a Delta IV 4050 Heavy, as well as a Star 48 V upper stage (2455 kg). The launch vehicle puts the spacecraft into geosynchronous transfer orbit (GTO), and the Star 48 V provides the apogee burn to produce a final geosynchronous orbit. We further note that more-optimal designs of several subsystems could potentially result in mass savings of at least several hundred kilograms.

Cost

A rough-order cost estimate for the GESS geosynchronous SAR mission concept was derived from Team X cost models and technology projections. With a technology cutoff year of 2010, a 5-year development, and 15-year mission operations, the total cost for the first satellite is in the range of $1–2 billion. A ten-satellite constellation will cost roughly $8–10 billion.

Future Opportunities

Seismology from Space Using Ka-Band GEO Satellite

Broadband digital seismometers — the current state of the art in seismology — offer continuous three-component surface displacements with sensitivities in the micron range. Although much of the world is covered with varying densities of broadband seismometers, they remain isolated to discrete point locations.

A satellite-based, continuous measurement of surface displacements with temporal and spatial sensitivities appropriate for seismic waves (submillimeter displacements, 0.01–1-Hz sampling) would represent an important step forward in understanding earthquake physics and solid Earth structure and dynamics. Current models for 3-D velocity structure of the

Earth are based on propagation of seismic waves as measured at discrete points. Spatially continuous mapping of seismic wave phases from large earthquakes would allow great improvements in crustal and lithospheric heterogeneity models, and would be synergistic with current developments in super computing models of 3-D Earth structure and seismic wave propagation (Figure 4.8). Detailed images of complex wave interference would generate significant improvements in basin seismic resonance and earthquake hazard assessment. By seeing the rupture unfold and observing the amplitudes of the seismic waves generated along the rupture, more-precise models would be determined for the rupture dynamics. This should lead to a fundamental improvement in our knowledge of how earthquakes initiate and why they stop.

The development of a radar mission for monitoring seismic waves involves tremendous technical challenges, but it is not outside the realm of possibility as a long-term goal. For now, we assume that the science requirements for such a mission dictate a horizontal resolution of 10 km, a vertical resolution of 100 μm, and a temporal resolution sufficient for following 5 km/s seismic waves.

While most spaceborne imaging radars employ aperture synthesis techniques for obtaining high horizontal resolution, the high-temporal resolution and wide-area coverage requirement of this application preclude the use of such techniques. That is, temporal sampling must occur on time scales finer than those possible for a high-altitude sensor to traverse a synthetic aperture length. Low-altitude sensors would be unable to provide sufficient coverage. We consequently envision a geostationary, real-aperture Ka-band system. That is, in contrast to the geosynchronous SAR, this platform must be maintained so that it does not move relative to the Earth surface. A constellation of three to five satellites could provide coverage for all equatorial and moderate-latitude regions of the Earth.

A short wavelength is desired so as to maximize the interferometric sensitivity to small surface displacements and to minimize the required antenna area, but the frequency must not be so great as to cause pulse-to-pulse decorrelation through frequency drift. We select the Ka-band frequency of 35 GHz (8.57-mm wavelength) for this analysis as a compromise. Therefore, in order to obtain 10-km horizontal resolution at a latitude of ±60°, an antenna with a diameter of approximately 110 m is required.

Assuming nominal system parameters, the high antenna gain implies that the single-pulse SNR will be greater than 40 dB for incidence angles up to 68° with 50 kW of radiated power and a normalized backscatter coefficient σ_0 of −20 dB. For this computation, we assume that a 1-μs gated continuous wave (CW) pulse is transmitted. (Range resolution is not required, as successive pulses are to be interferometrically combined.) Thermally induced phase noise will be much less than the 2.2° (25 dB SNR) threshold required for an interferometric vertical accuracy of 100 μm.

Successive pulses for each 10 km ground cell will need to be spaced by approximately 1 s if the wave speed is 5 km/s. Given the time between pulses, tropospheric artifacts may pose a significant limitation on the achievable vertical accuracy of the system (see Chapter 5, Optimizing the Measurement). Over 1 s, the tropospheric delay can vary by approximately 100 μm or more, depending on local condi-

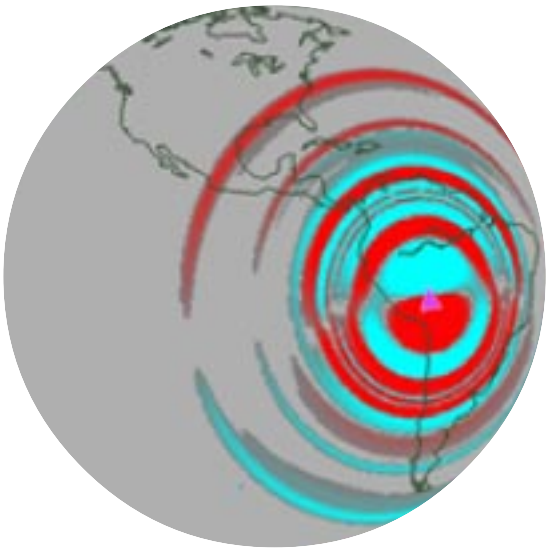

Figure 4.8
Modeled propagation of seismic waves from the deep, magnitude 8.2 Bolivia earthquake of June 9, 1994. The earthquake was so large that it produced a permanent displacement of the surface of the Earth of several millimeters near the epicenter in Bolivia. (Komatitsch and Tromp, 2002)

tions. Another factor limiting the system's vertical accuracy may be pulse-to-pulse decorrelation caused by changes of the ground surface between pulses; for example, from disturbances of the local vegetation by the wind. This effect will depend on the scene and its dominant scattering mechanisms at Ka-band. Moreover, it is not clear how the scattering centers of surface features such as vegetation move in response to a seismic wave propagating through the ground.

The total surface area that can be observed by the system during a seismic event is determined by the number of resolution cells that can be scanned within the interferometric repeat time of one second. We assume that the radar antenna is electronically steered to transmit pulses towards different ground cells at a 30-kHz pulse repetition frequency (PRF) during a transmit window equal to the 0.25-s round-trip pulse travel time. The radar then receives each of the transmitted pulses in turn. The total area covered in 1 second is approximately 10^{12} m^2, equivalent to a 1200-km-diameter circle.

The most important technological hurdle for such a system will likely be the design, construction, and deployment of a large, high-frequency antenna capable of fast, accurate electronic steering. Advanced onboard processing hardware and algorithms will also be required since the system must detect and respond adaptively to seismic events in real time. Stringent requirements may also be placed on spacecraft control and pointing given the solar pressure exerted on the large antenna.

Note that if the horizontal resolution were relaxed from 10 km to 30 km, the antenna diameter could be reduced by a factor of three, and the area coverage rate would increase by a factor of nine.

National Aeronautics and
Space Administration

Jet Propulsion Laboratory
California Institute of Technology
Pasadena, California

JPL 400-1069 03/03